USGS
science for a changing world

In cooperation with the University of Waterloo, Canada

Application of Advanced Geophysical Logging Methods in the Characterization of a Fractured-Sedimentary Bedrock Aquifer, Ventura County, California

by John H. Williams, John W. Lane, Jr., Kamini Singha, and F. P. Haeni

An integrated suite of advanced geophysical logging methods was used to characterize the geology and hydrology of three boreholes completed in fractured-sedimentary bedrock in Ventura County, California. The geophysical methods included caliper, gamma, electromagnetic induction, borehole deviation, optical and acoustic televiewer, borehole radar, fluid resistivity, temperature, and electromagnetic flowmeter. The geophysical logging 1) provided insights useful for the overall geohydrologic characterization of the bedrock and 2) enhanced the value of information collected by other methods from the boreholes including core-sample analysis, multiple-level monitoring, and packer testing.

The logged boreholes, which have open intervals of 100 to 200 feet, penetrate a sequence of interbedded sandstone and mudstone with bedding striking 220 to 250 degrees and dipping 15 to 40 degrees to the northwest. Fractures intersected by the boreholes include fractures parallel to bedding and fractures with variable strike that dip moderately to steeply. Two to three flow zones were detected in each borehole. The flow zones consist of bedding-parallel or steeply dipping fractures or a combination of bedding-parallel fractures and moderately to steeply dipping fractures. About 75 to more than 90 percent of the measured flow under pumped conditions was produced by only one of the flow zones in each borehole.

U.S. Department of the Interior
U.S. Geological Survey

WRIR 00-4083
March 2002

INTRODUCTION

Recent advances in geophysical logging methods have provided the opportunity to refine our understanding of ground-water flow and contaminant transport in fractured-bedrock aquifers. Integration of these new methods with conventional logging techniques can be used to define flow zones, lithology, and structure, and their relations in fractured bedrock. The purpose of this study is to demonstrate the application of an integrated suite of geophysical logs as part of the geohydrologic characterization of a fractured-sedimentary bedrock aquifer.

This study was done in cooperation with the University of Waterloo, Canada as part of an investigation of trichloroethene contamination in fractured sandstone and mudstone at the Rocketdyne Santa Susana Field ,, in southern Ventura County, California (fig. 1). The boreholes logged in this investigation were drilled as part of a ground-water flow and quality characterization study that included core-sample analysis, multiple-level monitoring, and packer testing (Sterling, 1999). Advanced geophysical logging methods were used to determine the geohydrologic character of flow zones in three boreholes including identification of lithology and location and orientation of bedding and fractures. This report includes a description of the geophysical logging methods and presents an integrated analysis of the geophysical logs.

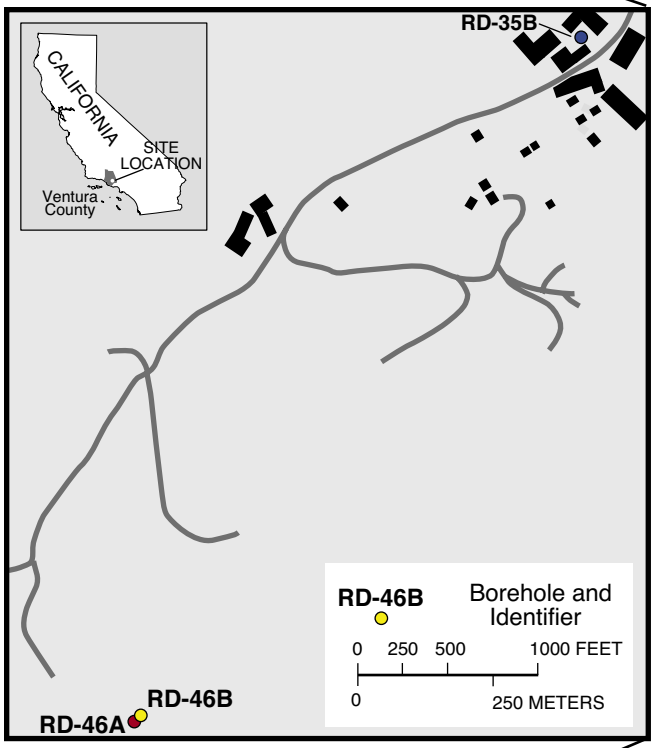

Figure 1. Location of Rocketdyne Santa Susana Field Laboratory and logged boreholes, southern Ventura County, California.

GEOPHYSICAL LOGGING METHODS

Geophysical logging methods used in this investigation included caliper, gamma, electromagnetic (EM) induction, borehole deviation, optical televiewer (OTV), acoustic televiewer (ATV), borehole radar, fluid resistivity, temperature, and EM flowmeter. The geophysical logging was done from December 2 to 4, 1998, and all logs were referenced to depth below top of casing. The logs were analyzed as an integrated suite to take full advantage of their synergistic nature.

Caliper logging records borehole diameter by use of a three-arm, spring-loaded tool (Keys, 1990). Changes in borehole diameter are related to drilling and construction procedures, caving in of less competent rocks, and the presence of fractures. The caliper logs were used with the OTV, ATV, fluid resistivity, temperature, and EM-flowmeter logs to characterize flow zones intersected by the boreholes.

Gamma logging records the amount of gamma radiation emitted by the rocks surrounding the borehole (Keys, 1990). The most significant naturally occurring sources of gamma radiation are potassium-40 and daughter products of the uranium- and thorium-decay series. Clay-bearing rocks commonly emit relatively high gamma radiation because they include weathering products of potassium feldspar and mica and tend to concentrate uranium and thorium by ion absorption and exchange. The vertical resolution of the gamma probe is 1 to 2 feet (ft). The gamma logs were used along with OTV and EM-induction logs to delineate the lithologic units intersected by the boreholes.

Electromagnetic-induction logging records the electrical conductivity, or resistivity, of the rocks and water surrounding the borehole (Williams and others, 1993). Electrical conductivity and resistivity are affected by the porosity and clay content of the rocks and by the dissolved solids concentration of the water in the rocks. The induction probe is designed to maximize vertical resolution and radial penetration and to minimize the effects of the borehole fluid. The induction probe has a vertical resolution of about 2 ft. In boreholes with diameters of 6 inches (in) or less, borehole fluid resistivity has a negligible effect on the induction-log response. The induction logs were used for lithologic interpretation and in delineation of possible changes in porosity or dissolved-solids concentration of the water in the rock matrix.

Borehole-deviation logging records the three-dimensional geometry of a borehole (Keys, 1990). Knowledge of borehole deviation is important to determine the true location and orientation of features intersected by the borehole. Borehole deviation tools generally indicate borehole inclination to within +/- 0.5° and direction to within +/- 2°. The borehole-deviation data were used to correct the orientation of lithologic features and fractures identified on the OTV and ATV logs.

Optical-televiewer logging records a magnetically oriented, 360° optical image of the borehole wall (Williams and Lane, 1998). An OTV log can be viewed as an unwrapped image similar to the traditional presentation of acoustic-televiewer data or it can be wrapped and viewed as a “virtual core”. The OTV can be used in air or below the borehole water level if the water has low turbidity. The vertical and horizontal sampling intervals for the OTV images were 0.01 and 0.008 in, respectively. Fractures and other planar features nearly as small as the sampling interval can be identified and characterized. The OTV logs were analyzed with the caliper, gamma, and EM-induction logs to identify lithology and determine the character and orientation of bedding and fractures. Bedding included bedding traces and lithologic contacts. Fractures included bedding-plane separations, joints, shear planes, and other planar breaks in the bedrock. The drilling process commonly causes bedrock adjacent to fractures to break out thereby increasing the apparent widths of fracture openings as viewed on borehole-wall images. Fractures with apparent opening widths of 0.1 in or more were classified as open or partially open.

Acoustic-televiewer logging records a magnetically oriented, 360° acoustic image of the borehole wall (Zemanek and others, 1969). The ATV is not affected by the clarity of the borehole water. The vertical sampling interval for the ATV images was 0.24 in. Fractures with apparent opening widths greater than 0.1 in can be detected on the ATV images. The ATV logs were used in combination with the OTV logs to determine the character and orientation of fractures.

Borehole-radar reflection logging records reflected wave amplitude and transit time of high-frequency EM waves using a pair of downhole transmitting and receiving antennas (Lane and others, 1994). A 100-megahertz non-directional radar system was used in this investigation. Borehole-radar reflection data are interpreted to determine the location and dip of fractures and lithologic changes, and to estimate the radial extent of such features beyond the borehole. The radar system used in this study cannot resolve fractures spaced closer than about 0.75 ft apart. The penetration of the radar signal is dependent on the electrical resistivity of the rock and water surrounding the borehole. Radial penetration in electrically resistive rocks (greater than 500 ohm-meters) may be more than 30 ft. The relatively low electrical resistivity of the sedimentary bedrock logged in this investigation (near 100 ohm-meters) limited radial penetration to less than 10 ft.

Fluid-resistivity logging records the electrical resistivity of the water in a borehole (Williams and Conger, 1990). The electrical resistivity of the water is related to its dissolved-solids concentration. Fluid-resistivity logs were collected under ambient and pumped conditions. The fluid-resistivity logs were combined with the temperature and flowmeter logs to identify flow zones and to determine the relative dissolved-solids concentration of their contained water.

Temperature logging records the temperature of the water in the borehole (Williams and Conger, 1990). In boreholes with no vertical borehole flow, the temperature of the borehole water generally increases with depth as a function of the geothermal gradient in the surrounding rocks. Temperature gradients less than the geothermal may indicate intervals with vertical borehole flow. Temperature logs were used with the fluid-resistivity and EM-flowmeter logs to identify flow zones under ambient and pumped conditions.

Electromagnetic-flowmeter logging records the direction and rate of vertical flow in a borehole. The flow of water (an electrical conductor) through an induced magnetic field generates a voltage gradient that according to Faraday's Law is proportional to its velocity (Young and Pearson, 1995). Stationary flow measurements were made under ambient conditions and both trolling and stationary measurements were made under pumped conditions. Tool measurement drift is approximately plus or minus 0.1 gallons per minute (gal/min) without a flow restrictor in 3-in diameter holes and plus or minus 0.03 gal/min with a flow restrictor in 6-in diameter holes. Through a comparison with straddle-packer testing, Paillet (1998) showed that the flowmeter-logging method consistently detected flow zones with transmissivity values that have the same order of magnitude as the most productive zone in the borehole. In addition, about half of the flow zones with transmissivity values an order of magnitude less than the most productive zone were detected and less than 20 percent of the zones with transmissivity values two orders of magnitude less were detected. The EM-flowmeter logs were used in conjunction with the fluid-resistivity and temperature logs to identify flow zones, commonly composed of multiple fractures, and their relative hydraulic head, flow contribution, and dissolved-solids concentration.

Borehole RD-35B is cased with steel to a depth of 163 ft and completed as a 3-in diameter open hole to a depth of 360 ft. The borehole is at north latitude 34°14′08″ and west longitude 118°40′30″. Top of casing is 1,905.7 ft above sea level. The ambient water level in the borehole during the logging period was at a depth of 63.5 ft. Integrated analysis of the OTV, gamma, and EM-induction logs indicates that the borehole intersects a sequence of sandstone and mudstone (figs. 2 and 3) as follows:

Depth, in ft	Lithology
163-201	Sandstone
201-202	Mudstone
202-233	Sandstone
233-260	Sandstone and mudstone
260-301	Sandstone
301-316	Mudstone and sandstone
316-360	Sandstone

The sandstone had higher resistivity and radar velocity and lower gamma than the mudstone. The resistivity of the sandstones below 278 ft is lower than the resistivity of the sandstones above this depth (fig. 2). The gamma logs do not indicate an increase in clay content in the lower sandstones. Therefore, the decrease in resistivity observed in the sandstones below 278 ft is related to an increase in the dissolved-solids content of the matrix water and (or) an increase in matrix porosity.

The character and orientation of bedding and fractures in borehole RD-35B were determined from the analysis of the OTV, ATV, and borehole-radar velocity logs (table 1 and fig. 4). Bedding generally strikes 220 to 260° and dips 15 to 30° to the northwest. Fractures in RD-35B include:

(1) 15 fractures that parallel bedding;
(2) 7 moderately dipping fractures that generally strike 200 to 215°; and
(3) 19 steeply dipping fractures that generally strike 0 to 230°.

Thirty-one of the 41 fractures appear open or partially open with maximum apparent opening widths that range from 0.1 to 3.8 inches.

Integrated analysis of the EM-flowmeter, fluid-resistivity, and temperature logs with the OTV and ATV logs indicates that the borehole intersected flow zones at 201 and 312 ft (fig. 5). The flow zone at 201 ft (fig. 6) is coincident with a thin mudstone unit within a 65-ft thick sandstone sequence. This zone consists of five fractures that strike about 200 to 230° and dip 20 to 60° to the northwest. The flow zone at 312 ft (fig. 7) is within interbedded sandstone and mudstone and consists of a bedding-parallel fracture and five steeply dipping fractures. The 201- and 312-ft flow zones appear on the borehole radar logs as intervals of low radar velocity (fig. 4).

Analysis of the fluid-resistivity, temperature, and EM-flowmeter logs (fig. 5) suggests that slight downward flow occurs in borehole RD-35B under ambient conditions. Water enters RD-35B at the 201-ft flow zone, exiting at the 312-ft flow zone. The measured downward-flow rate is within the tool measurement drift of the EM flowmeter when used without a flow restrictor. The more definitive evidence for downward flow is indicated by a comparison of the fluid-resistivity logs under ambient conditions when flow is downward and pumped conditions when flow is upward. The presence of downward flow indicates that the 201-foot flow zone has a higher hydraulic head than the 312-ft zone.

RD-35B was pumped at 4.9 gal/min for 1.5 hours (h). The specific capacity of the well was 0.46 (gal/min)/ft with a drawdown of 10.7 ft. About 75 percent of the flow measured under pumped conditions was produced by the 201-ft zone; the remaining 25 percent was produced by the lower zone. Borehole fluid-resistivity logs under ambient and pumped conditions indicate that the 312-ft zone produces water that has a lower fluid resistivity (higher dissolved-solids content) than the 201-ft zone. Repeated fluid-resistivity logs illustrate that water in the borehole above the flow zones was purged between 0.5 and 1.5 h after the start of pumping.

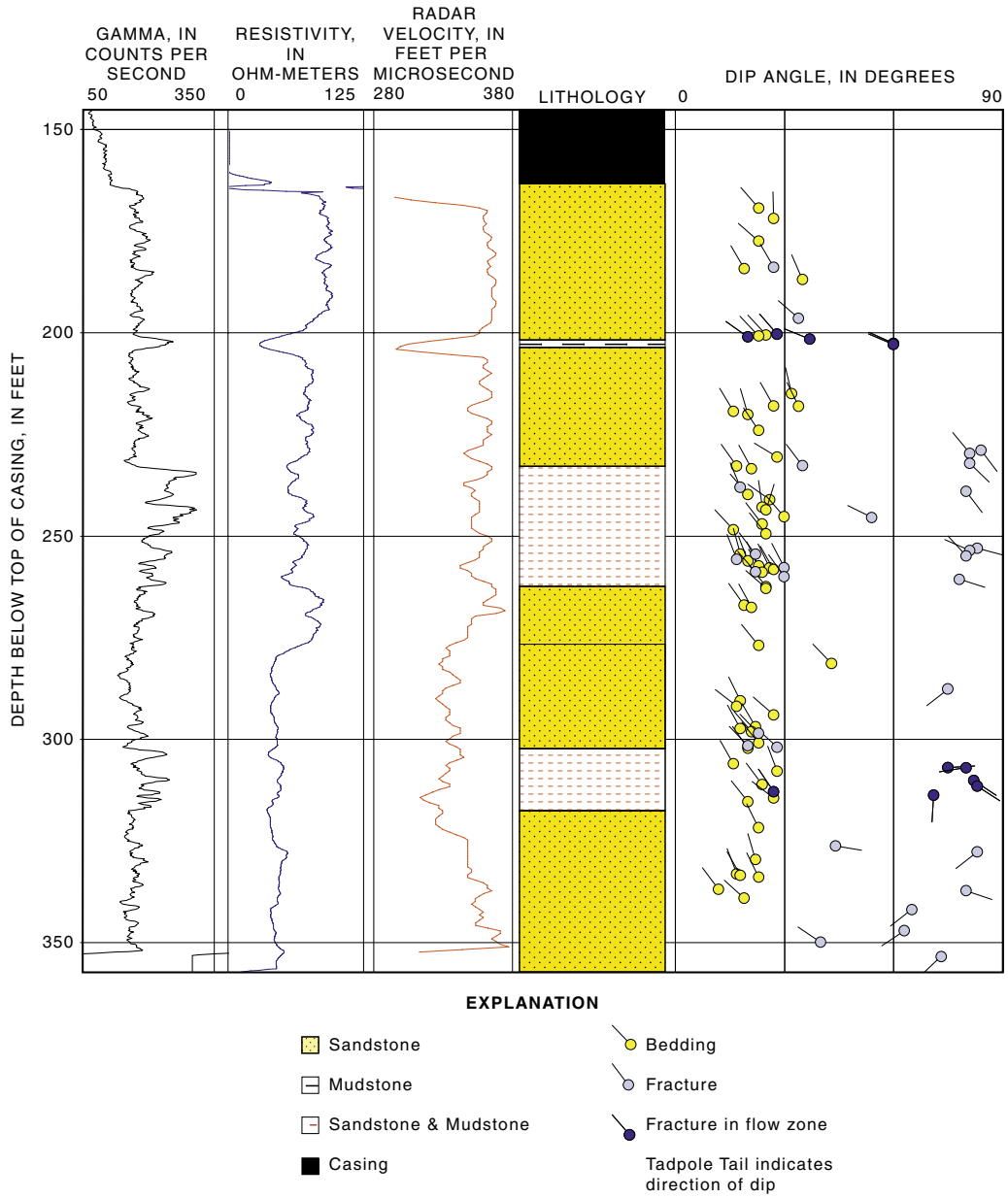

Figure 2. Gamma, resistivity, radar velocity, lithology, and bedding and fracture orientations for borehole RD-35B, Rocketdyne Santa Susana Field Laboratory, Ventura County, California.

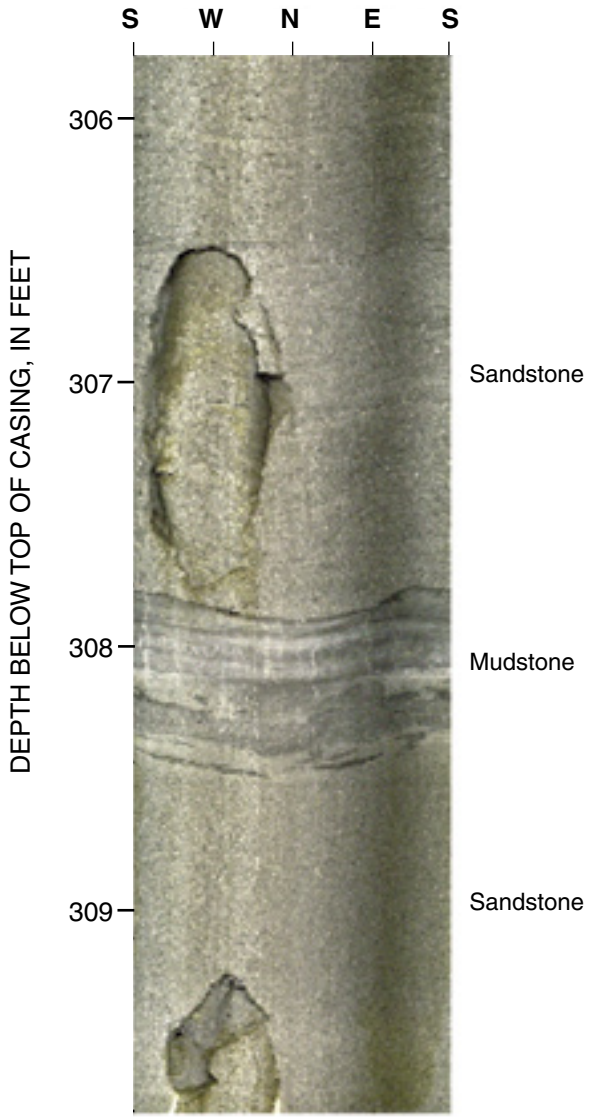

Figure 3. Optical-televiewer image of sandstone and mudstone in borehole RD 35B, Rocketdyne Santa Susana Field Laboratory, Ventura County, California.

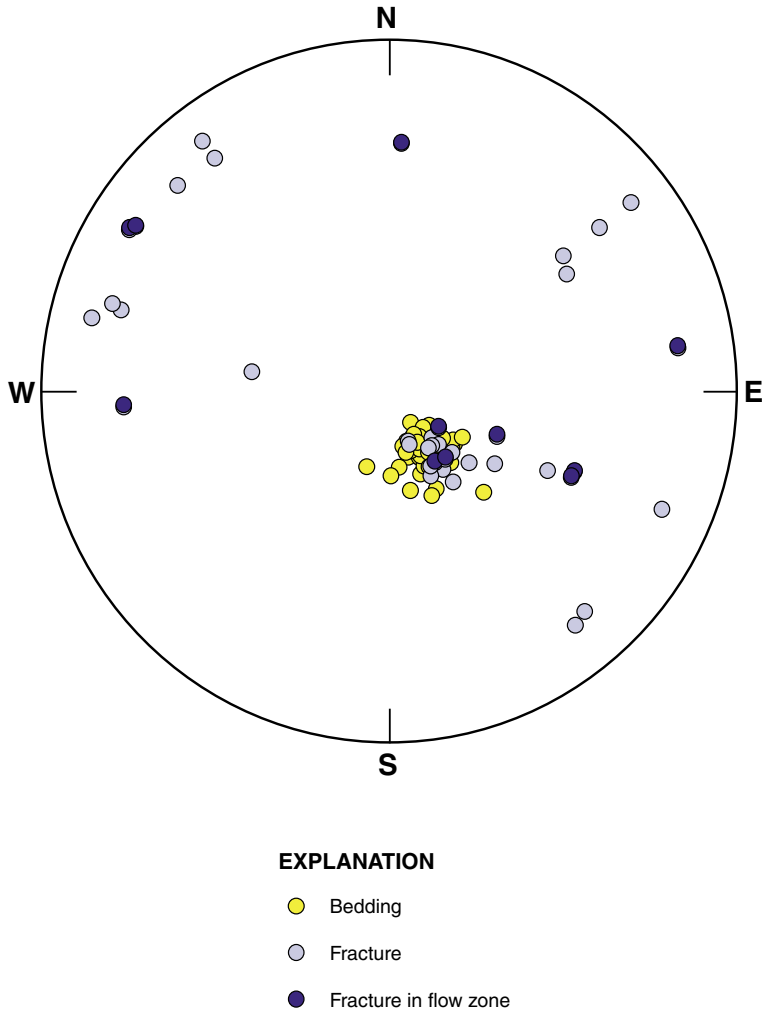

Figure 4. Lower-hemisphere, equal-area projection (stereogram) of poles for bedding and fractures in borehole RD-35B, Rocketdyne Santa Susana Field Laboratory, Ventura County, California.

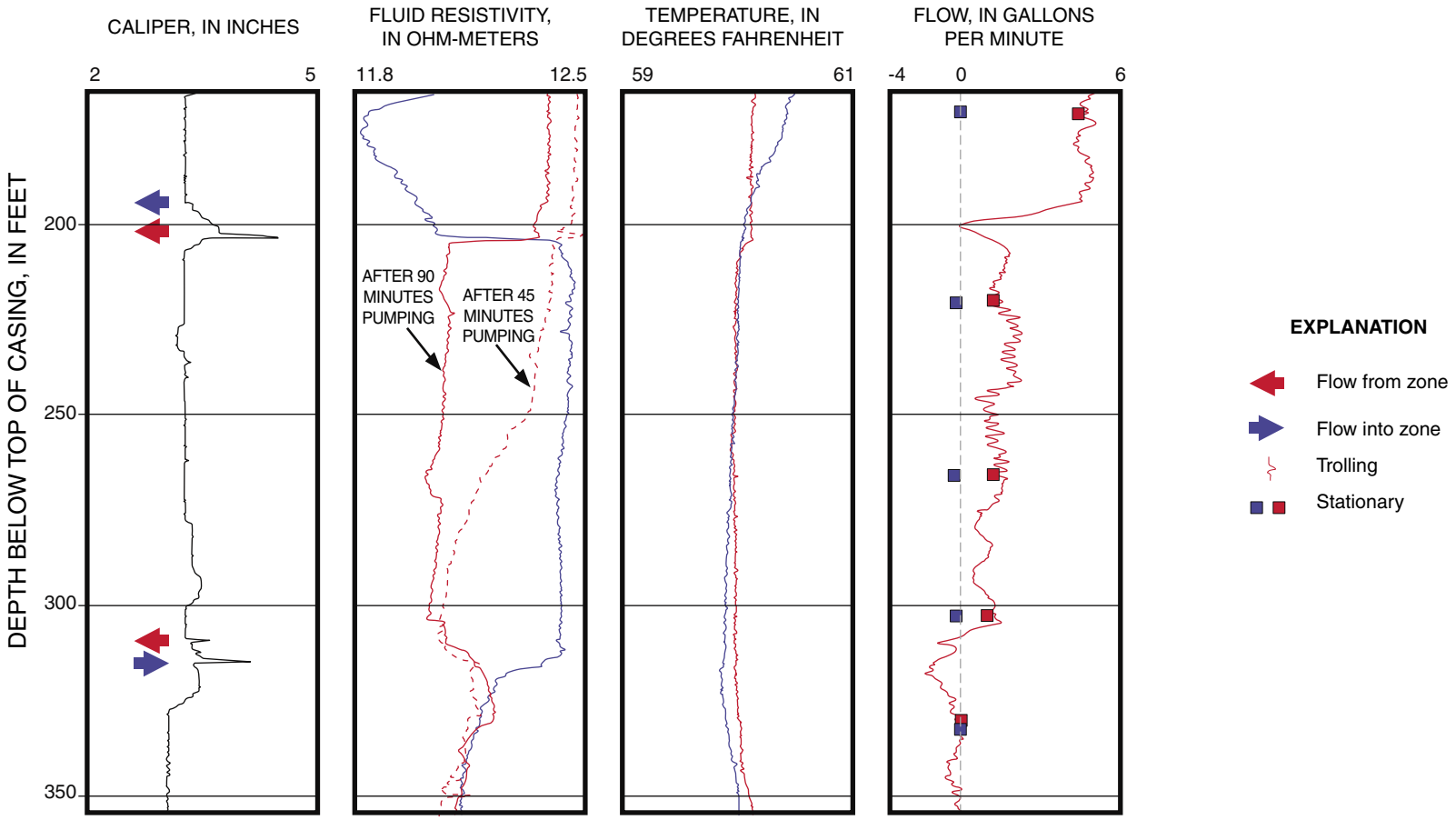

Figure 5. Caliper, fluid-resistivity, temperature, and flowmeter logs of borehole RD-35B, Rocketdyne Santa Susana Field Laboratory, Ventura County, California (arrows indicate flow zones; blue indicates ambient conditions, red indicated pumped conditions; negative values indicate downflow, positive values indicate upflow).

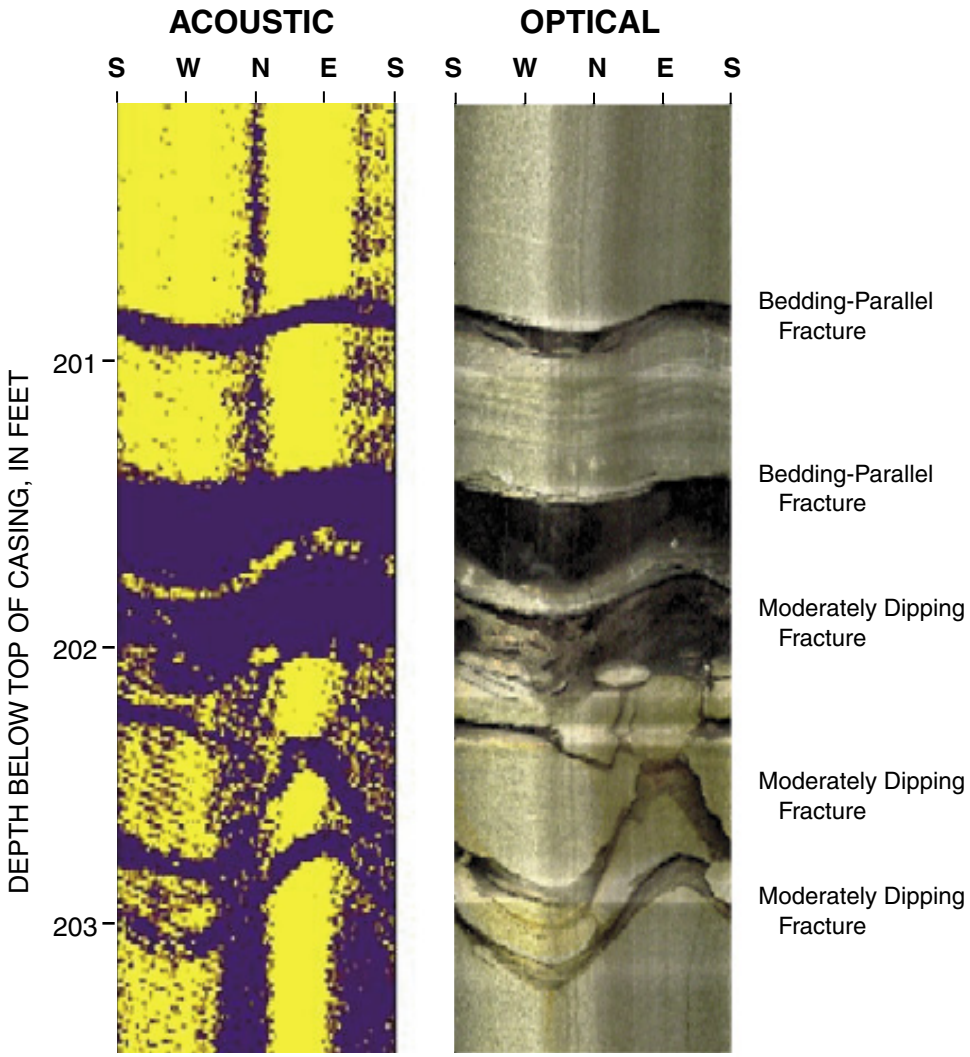

Figure 6. Acoustic- and optical-televiewer images of the flow zone near 201 feet in borehole RD-35B, Rocketdyne Santa Susana Field Laboratory, Ventura County, California.

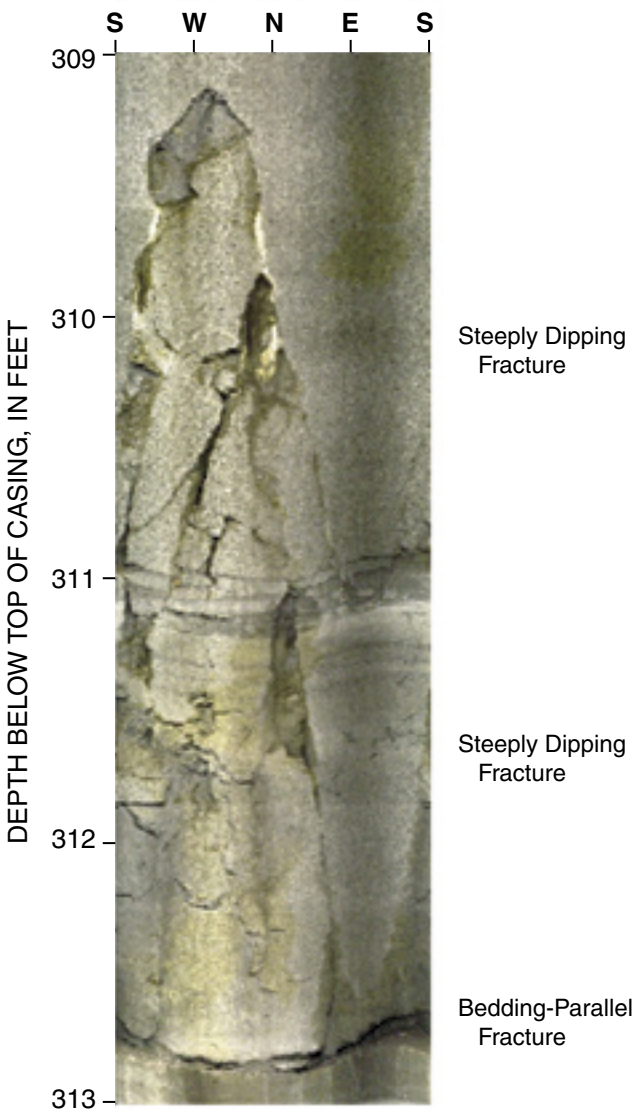

Figure 7. Optical-televiewer image of the flow zone near 312 feet in borehole RD-35B, Rocketdyne Santa Susana Field Laboratory, Ventura County, California.

Table 1. Midpoint depth, strike, and dip of bedding and fractures penetrated by borehole RD-35B, Rocketdyne Santa Susana Field Laboratory, Ventura County, California

[Strike is reported in azimuthal degrees, east of True North in "right hand rule" where the direction of the dip is to the right of the strike; blue indicates fractures in flow zones;-- indicates not determined.]

No.	Midpoint depth from top of casing, in feet	Type	Strike, in degrees	Dip, in degrees	Maximum apparent aperture, in inches
1	169.3	Bedding	229	23	--
2	171.9	Bedding	269	27	--
3	177.4	Bedding	221	23	--
4	183.9	Fracture	240	27	0.2
5	184.2	Bedding	240	19	--
6	186.8	Bedding	247	35	--
7	196.5	Fracture	221	34	0.1
8	200.4	Fracture	229	28	1.2
9	200.5	Bedding	228	25	--
10	200.8	Bedding	227	23	--
11	201.1	Fracture	215	20	3.8
12	201.5	Fracture	202	37	2.8
13	202.6	Fracture	205	60	0.2
14	202.9	Fracture	203	60	0.2
15	215.1	Bedding	257	32	--
16	218.0	Bedding	241	27	--
17	218.1	Bedding	244	34	--
18	219.3	Bedding	239	16	--
19	220.0	Bedding	254	20	--
20	224.0	Bedding	237	23	--
21	228.8	Fracture	53	84	--
22	229.7	Fracture	231	81	--
23	230.5	Bedding	211	28	--
24	232.1	Fracture	44	81	0.2
25	232.6	Fracture	234	35	--
26	232.8	Bedding	235	17	--
27	233.4	Bedding	242	21	--
28	238.0	Fracture	248	18	0.1
29	239.0	Fracture	53	80	0.1
30	239.7	Bedding	230	20	--
31	241.0	Bedding	216	26	--
32	242.9	Bedding	262	24	--
33	243.5	Bedding	288	25	--

Table 1. Midpoint depth, strike, and dip of bedding and fractures penetrated by borehole RD-35B, Rocketdyne Santa Susana Field Laboratory, Ventura County, California -- continued

[Strike is reported in azimuthal degrees, east of True North in "right hand rule" where the direction of the dip is to the right of the strike; blue indicates fractures in flow zones;-- indicates not determined.]

No.	Midpoint depth from top of casing, in feet	Type	Strike, in degrees	Dip, in degrees	Maximum apparent aperture, in inches
34	245.2	Bedding	229	30	--
35	245.4	Fracture	206	54	0.1
36	247.1	Bedding	233	24	--
37	248.4	Bedding	227	16	--
38	249.4	Bedding	232	25	--
39	253.0	Fracture	14	83	0.1
40	253.5	Fracture	203	81	0.1
41	254.4	Fracture	234	22	0.2
42	254.5	Bedding	255	18	--
43	254.9	Fracture	228	80	0.2
44	255.8	Bedding	252	14	--
45	255.8	Fracture	249	17	0.2
46	256.3	Bedding	249	20	--
47	257.3	Bedding	244	23	--
48	257.7	Fracture	243	30	0.1
49	257.9	Bedding	244	26	--
50	258.2	Bedding	241	27	--
51	258.8	Fracture	230	22	0.1
52	258.9	Bedding	239	24	--
53	259.9	Fracture	235	30	0.5
54	260.6	Fracture	17	78	0.3
55	262.5	Bedding	232	25	--
56	262.9	Bedding	221	25	--
57	267.1	Bedding	235	19	--
58	267.6	Bedding	242	21	--
59	276.9	Bedding	231	23	--
60	281.3	Bedding	226	43	--
61	287.7	Fracture	142	75	--
62	290.6	Bedding	244	18	--
63	291.8	Bedding	218	17	--
64	294.0	Bedding	221	27	--
65	296.8	Bedding	240	22	--
66	297.4	Bedding	242	18	--

Table 1. Midpoint depth, strike, and dip of bedding and fractures penetrated by borehole RD-35B, Rocketdyne Santa Susana Field Laboratory, Ventura County, California -- continued

[Strike is reported in azimuthal degrees, east of True North in "right hand rule" where the direction of the dip is to the right of the strike; blue indicates fractures in flow zones;-- indicates not determined.]

No.	Midpoint depth from top of casing, in feet	Type	Strike, in degrees	Dip, in degrees	Maximum apparent aperture, in inches
67	298.2	Bedding	229	21	--
68	298.6	Fracture	226	24	0.1
69	298.6	Fracture	226	23	0.1
70	301.0	Bedding	232	23	--
71	301.5	Fracture	226	20	0.1
72	301.9	Fracture	223	28	0.5
73	302.2	Bedding	235	20	--
74	306.0	Bedding	241	16	--
75	306.9	Fracture	357	75	0.2
76	307.0	Fracture	171	80	0.1
77	307.8	Bedding	249	28	--
78	310.1	Fracture	33	82	0.2
79	311.2	Bedding	234	24	--
80	311.5	Fracture	32	83	0.2
81	312.8	Fracture	237	27	0.8
82	313.8	Fracture	93	71	0.1
83	314.4	Bedding	218	27	--
84	315.3	Bedding	232	20	--
85	321.8	Bedding	245	23	--
86	326.2	Fracture	9	44	--
87	327.7	Fracture	142	83	--
88	329.5	Bedding	254	22	--
89	333.1	Bedding	250	17	--
90	333.4	Bedding	241	18	--
91	333.9	Bedding	245	23	--
92	336.9	Bedding	234	12	--
93	337.2	Fracture	18	80	--
94	339.1	Bedding	223	19	--
95	342.0	Fracture	142	65	--
96	347.1	Fracture	146	63	0.2
97	349.9	Fracture	214	40	--
98	353.4	Fracture	137	73	--

Borehole RD-46A is cased with steel to a depth of 32 ft and completed as a 6-in diameter open hole to a depth of 138 ft. The borehole is at north latitude 34°13′29″ and west longitude 118°41′00″.The top of casing is 1,806.1 ft above sea level. The ambient water level in the borehole during the logging period was at a depth of 66.4 ft. Analysis of the OTV log indicates the borehole intersects a sequence of sandstone and mudstone as follows:

Depth, in ft	Lithology
32-73	Sandstone and mudstone
73-76	Mudstone with some sandstone
76-124	Sandstone with some mudstone
124-129	Sandstone and mudstone (slumped/turbated)
129-138	Sandstone and mudstone

The character and orientation of bedding and fractures in borehole RD-46A were determined from the analysis of the OTV log (table 2 and figs. 8 and 9). Bedding generally strikes 235 to 260° and dips 20 to 35° to the northwest. Fractures in RD-46A include:

1) 5 fractures that parallel bedding; and
2) 9 steeply-dipping fractures that generally strike 30 to 75°.

Nine of the 14 fractures appear open or partially open with maximum apparent opening widths that range from 0.1 to 1.7 inches.

Integrated analysis of the fluid-resistivity, temperature, and EM-flowmeter logs with the OTV log indicates that the borehole intersects flow zones at 95, 119, and 132 ft (fig. 10). The flow zones at 95 ft (fig. 11) and at 119 ft (fig. 12) both consist of a steeply dipping fracture in sandstone. The zone at 132 ft (fig. 13) consists of a bedding-parallel fracture within a 0.5 ft thick mudstone interbed.

The EM-flowmeter log (fig. 10) indicates no measurable flow occurs in borehole RD-46A under ambient conditions. The diameter of borehole RD-46A (6 in) enabled the use of a flow restrictor during EM-flowmeter logging. The lack of measurable ambient flow indicates the presence of little vertical hydraulic gradient between flow zones and (or) the lack of more than one zone that can produce or receive detectable flow under the existing gradient.

RD-46A was pumped at 3.3 gal/min for 3 h. The specific capacity of the borehole was 0.55 (gal/min)/ft with a drawdown of 6.0 ft. More than 90 percent of the flow measured under pumped conditions was produced by the 95-foot zone, less than 5 percent was produced by the 119-ft zone, and less than 2 percent was produced by the 132-ft zone. Repeated fluid-resistivity logs collected during pumping indicated that water in the borehole above the flow zones was not purged after 3 h of pumping.

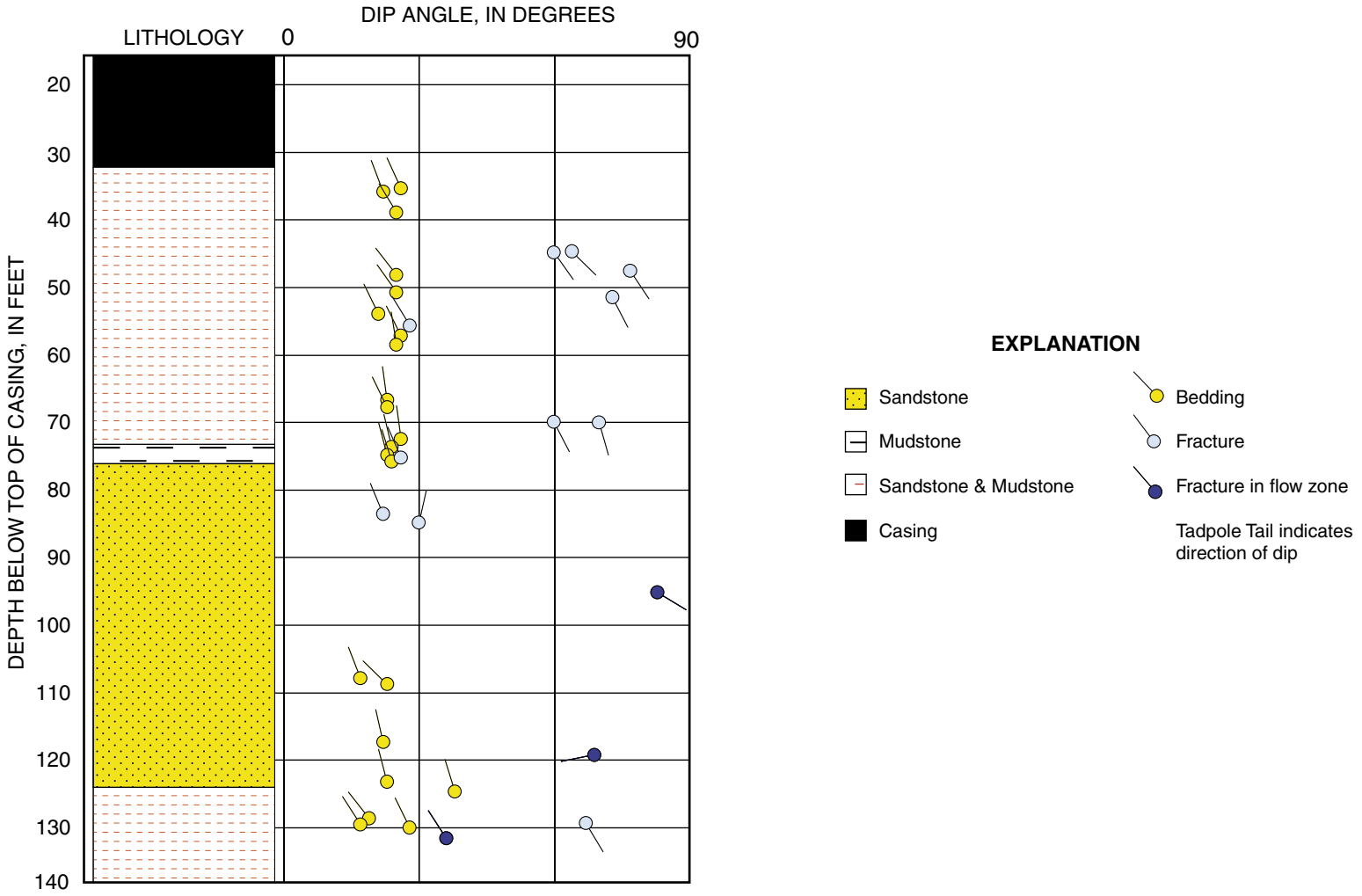

Figure 8. Lithology and bedding and fracture orientations in borehole RD-46A, Rocketdyne Santa Susana Field Laboratory, Ventura County, California.

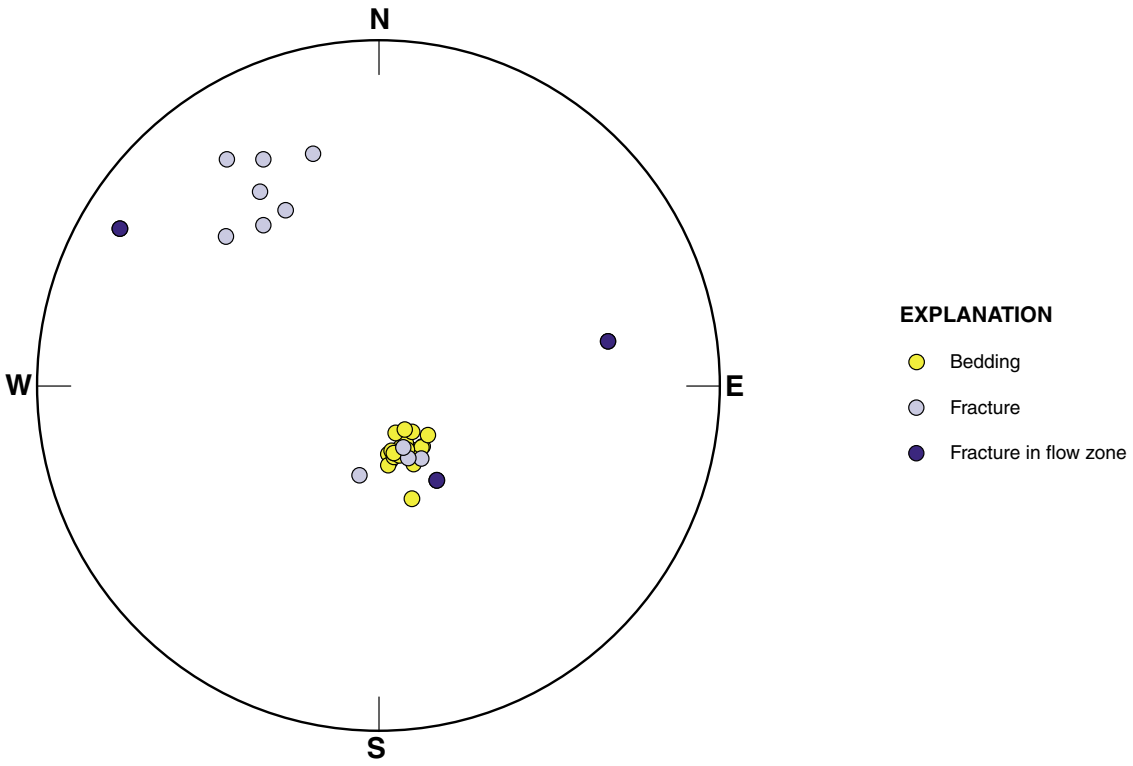

Figure 9. Lower-hemisphere, equal-area projection (stereogram) of poles for bedding and fractures in borehole RD-46A, Rocketdyne Santa Susana Field Laboratory, Ventura County, California.

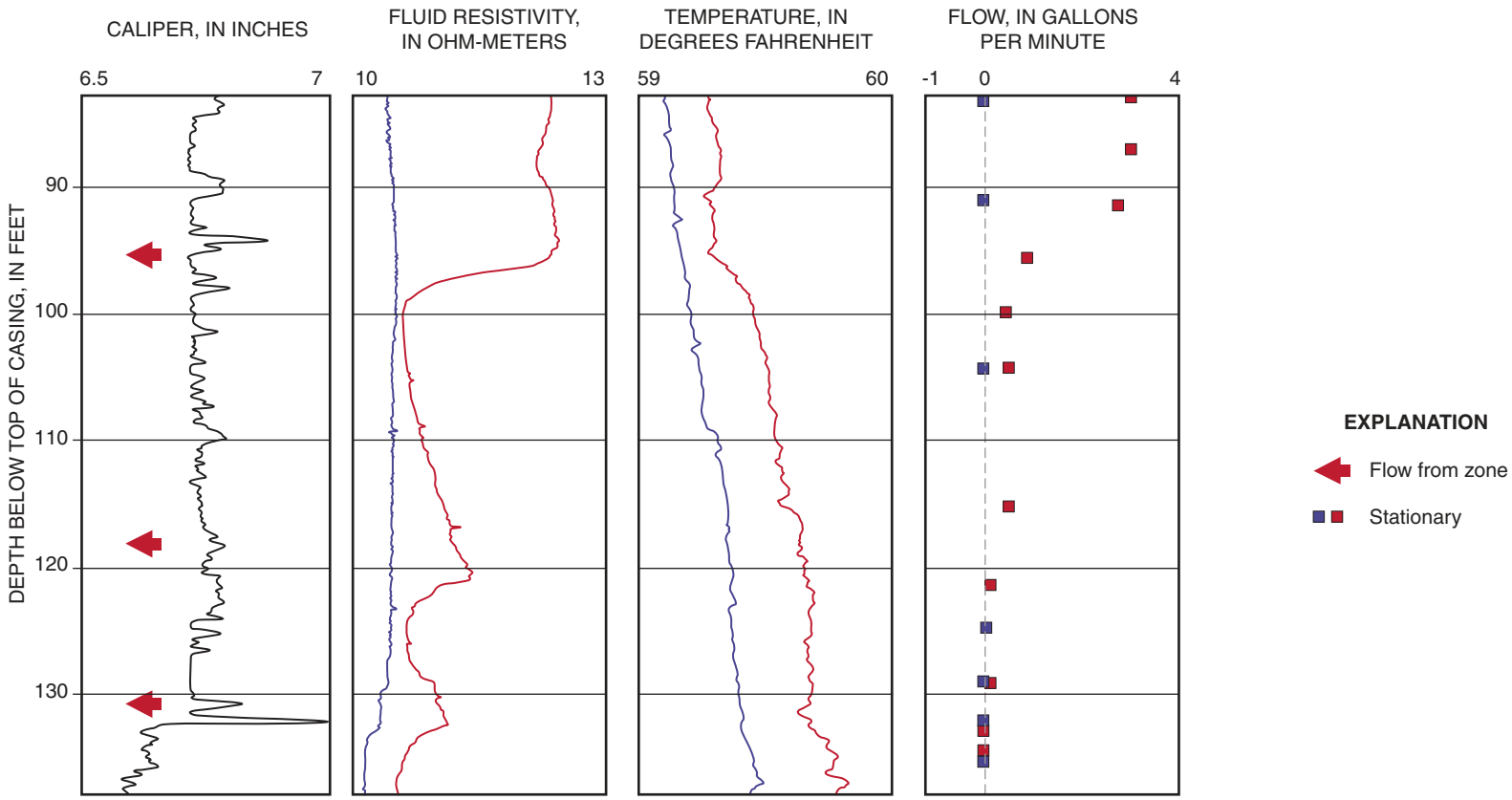

Figure 10. Caliper, fluid-resistivity, temperature, and flowmeter logs of borehole RD-46A, Rocketdyne Santa Susana Field Laboratory, Ventura County, California (arrows indicate flow zones; blue indicates ambient conditions, red indicates pumped conditions; negative values indicate downflow, positive values indicate upflow).

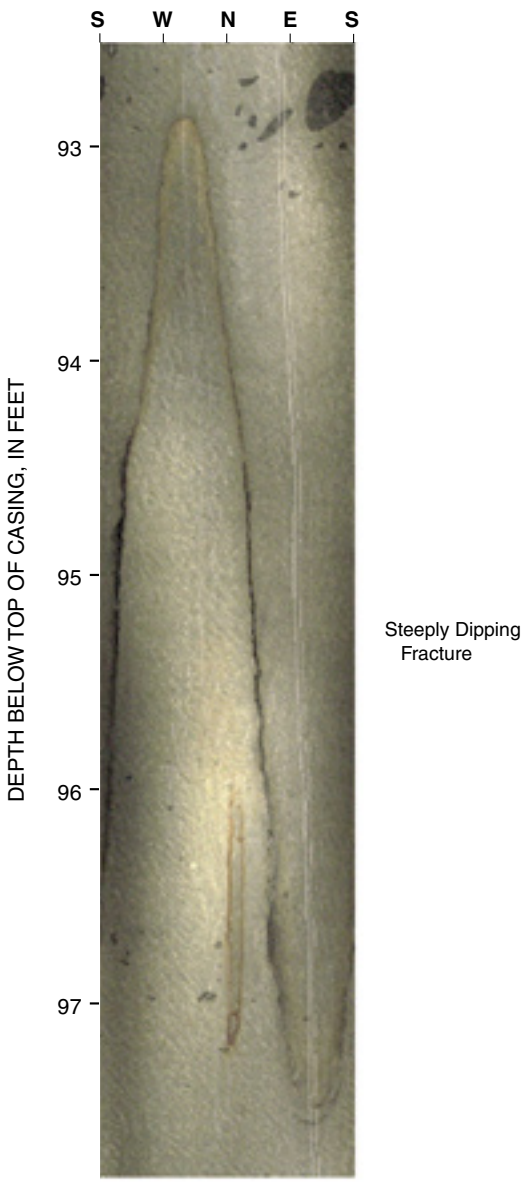

Figure 11. Optical-televiewer image of the flow zone near 95 feet in borehole RD-46A, Rocketdyne Sanat Susana Field laboratory, Ventura County, California.

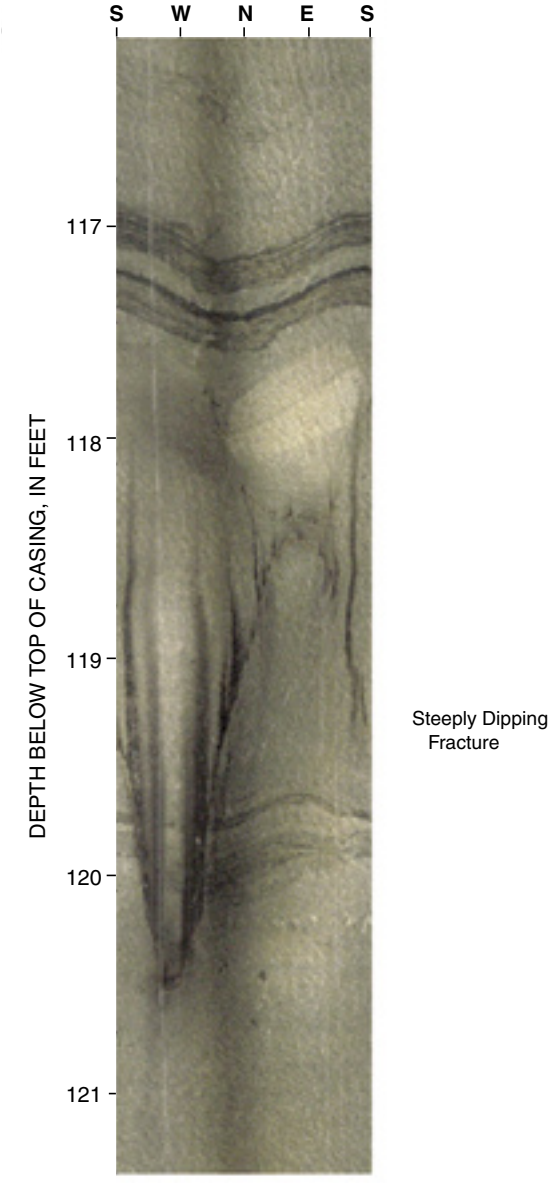

Figure 12. Optical-televiewer image of the flow zone near 119 feet in borehole RD-46A, Rocketdyne Sanat Susana Field laboratory, Ventura County, California.

Figure 13. Optical-televiewer image of the flow zone near 132 feet in borehole RD-46A, Rocketdyne Sanat Susana Field laboratory, Ventura County, California.

Table 2. Midpoint depth, strike, and dip of bedding and fractures penetrated by borehole RD-46A, Rocketdyne Santa Susana Field Laboratory, Ventura County, California

[Strike is reported in azimuthal degrees, east of True North in "right hand rule" where the direction of the dip is to the right of the strike; blue indicates fractures in flow zones;-- indicates not determined.]

No.	Midpoint depth from top of casing, in feet	Type	Strike, in degrees	Dip, in degrees	Maximum apparent aperture, in inches
1	35.3	Bedding	246	26	--
2	35.8	Bedding	250	22	--
3	38.9	Bedding	239	25	--
4	44.7	Fracture	44	64	0.2
5	44.8	Fracture	54	60	0.1
6	47.5	Fracture	56	77	--
7	48.1	Bedding	233	25	--
8	50.7	Bedding	235	25	--
9	51.5	Fracture	63	73	--
10	53.9	Bedding	244	21	--
11	55.6	Fracture	239	28	1.7
12	57.2	Bedding	245	26	--
13	58.6	Bedding	261	25	--
14	66.6	Bedding	262	23	--
15	67.7	Bedding	245	23	--
16	69.9	Fracture	62	60	--
17	70.0	Fracture	74	70	--
18	72.4	Bedding	263	26	--
19	73.6	Bedding	257	24	--
20	74.8	Bedding	256	23	--
21	75.2	Fracture	247	26	0.1
22	75.8	Bedding	253	24	--
23	83.6	Fracture	248	22	0.2
24	84.8	Fracture	283	30	0.2
25	95.2	Fracture	31	83	0.2
26	107.9	Bedding	250	17	--
27	108.8	Bedding	224	23	--
28	117.3	Bedding	258	22	--
29	119.2	Fracture	169	69	0.8
30	123.2	Bedding	256	23	--
31	124.6	Bedding	253	38	--
32	128.6	Bedding	233	19	--
33	129.3	Fracture	58	67	--
34	129.5	Bedding	238	17	--
35	130.0	Bedding	245	28	--
36	131.6	Fracture	238	36	0.4

Borehole RD-46B is cased with steel to a depth of 192 ft and completed as a 3-in diameter open hole to a depth of 364 ft. The borehole is at north latitude 34°13′29″ and west longitude 118°41′00″.Top of casing is at 1,807.2 ft above sea level. The ambient water level in the borehole during the logging period was at a depth of 48.4 feet. Integrated analysis of the OTV, gamma, and EM-induction logs (fig. 14) indicates the borehole intersects a sequence of sandstone and mudstone as follows:

Depth, in feet	Lithology
192-287	Sandstone with mudstone (interbeds and clasts)
287-296	Mudstone and sandstone
296-332	Mudstone with sandstone
332-336	Sandstone
336-358	Mudstone with sandstone
358-362	Sandstone with mudstone
362-364	Mudstone with sandstone

The character and orientation of bedding and fractures in borehole RD-46B were determined from the analysis of the OTV log (table 3 and figs. 14 and 15). Bedding generally strikes 230 to 250° and dips 20 to 40° to the northwest. Fractures in RD-46B include:

1) 27 fractures that parallel bedding;
2) 5 moderately dipping fractures that strike generally strike 130 to 260°; and
3) 7 steeply dipping fractures that have a wide range of strikes.

Thirty-three of 39 fractures appear open or partially open with maximum apparent opening widths that range from 0.1 to 0.7 inches.

Integrated analysis of the fluid-resistivity, temperature, and EM-flowmeter logs with the OTV log indicates the borehole intersects flow zones at 289 and 306 ft (fig. 16). The 289-ft zone is within a mudstone and sandstone sequence at the contact between the upper sandstone and the lower mudstone and sandstone units. This zone (fig. 17) consists of a series of four fractures that parallel bedding and a steeply dipping fracture. The 306-ft zone (fig. 18) consists of two bedding-parallel fractures and a steeply dipping fracture. Several other fractures that appear open intersect the borehole just below this flow zone: a fracture at 311 ft that dips 50°, and a series of bedding-parallel fractures at 313 ft.

The EM-flowmeter log (fig. 16), which was collected without a flow restrictor, indicates no measurable flow in borehole RD-46B under ambient conditions. However, a change in the gradient on the fluid temperature logs suggests that flow might be occurring at the 289-ft zone.

RD-46B was pumped at 4.8 gal/min for 2 h. The specific capacity of the borehole was 0.33 (gal/min)/ft with a drawdown of 14.4 ft. The zone at 289 ft produced about 80 percent of the flow measured under pumped conditions and the zone at 306 ft produced about 20 percent. The fluid-resistivity log under pumped conditions suggests that the 289- and 306-ft zones produced water with similar dissolved-solids content. Repeated fluid-resistivity logs indicated that the water in the borehole above the flow zones was purged within 0.75 h from the start of pumping.

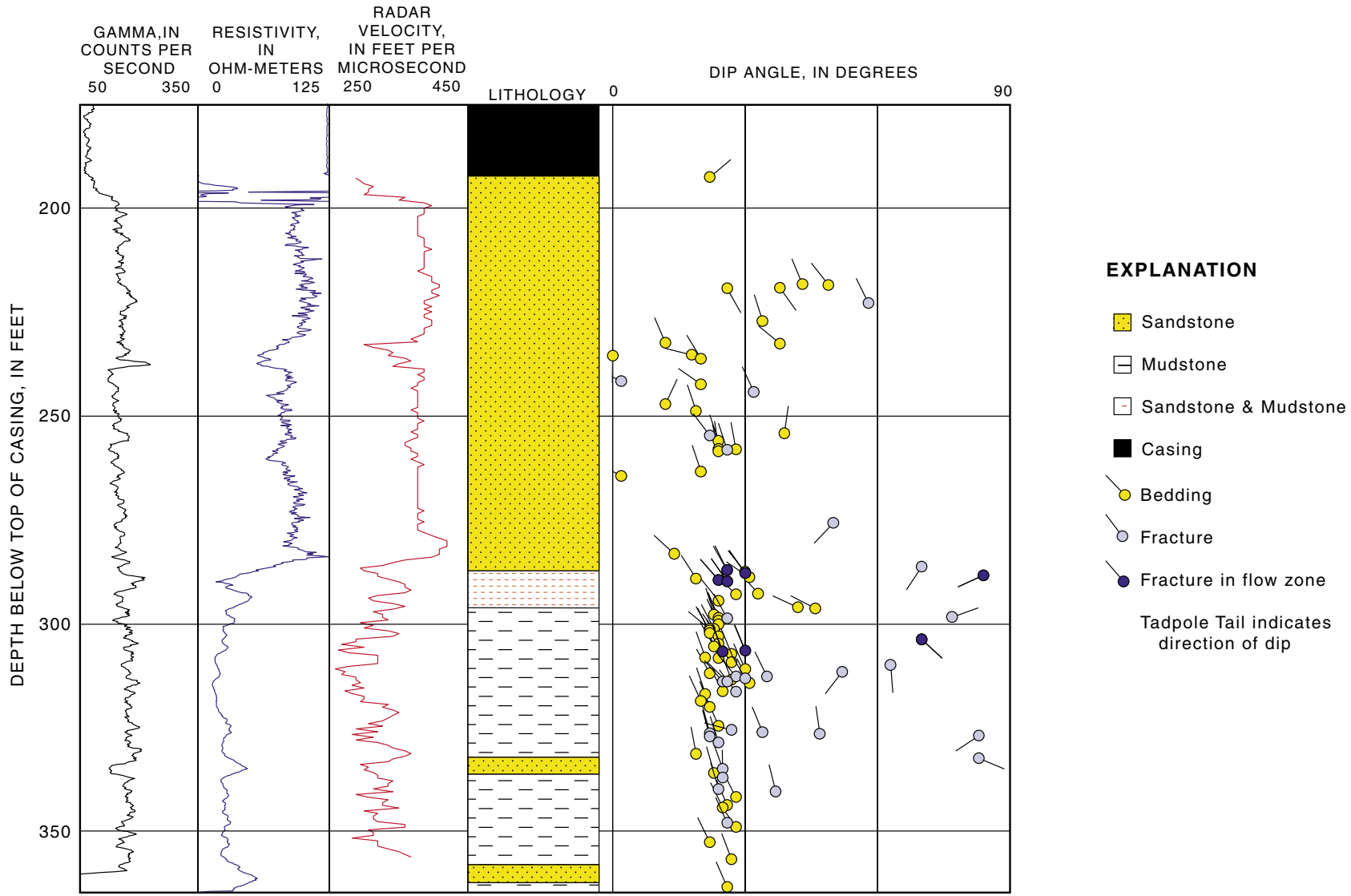

Figure 14. Gamma, resistivity, radar velocity, lithology, and bedding and fracture orientations for borehole RD-46B, Rocketdyne Santa Susana Field Laboratory, Ventura County, California.

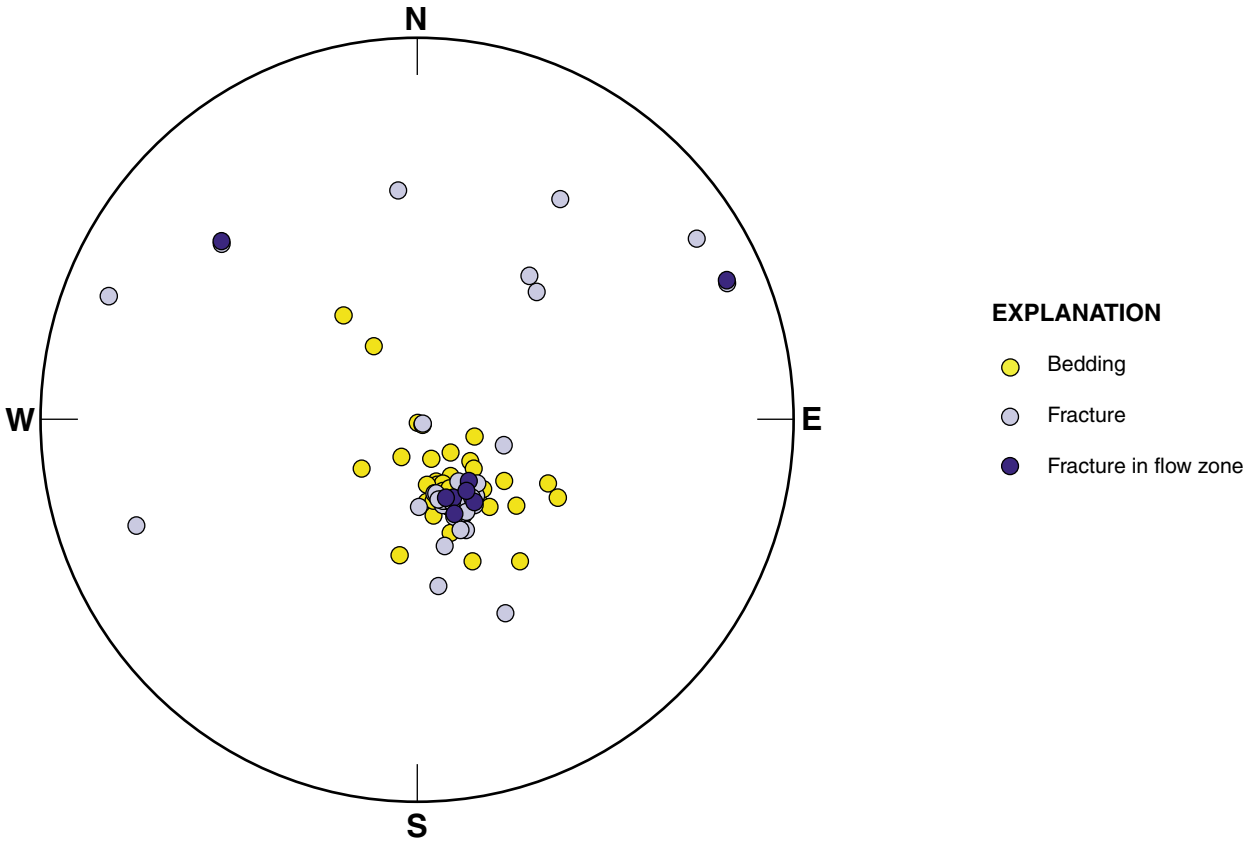

Figure 15. Lower hemisphere, equal-area projection (stereogram) of poles for bedding and fractures in borehole R46B, Rocketdyne Santa Susana Field Laboratory, Ventura County, California.

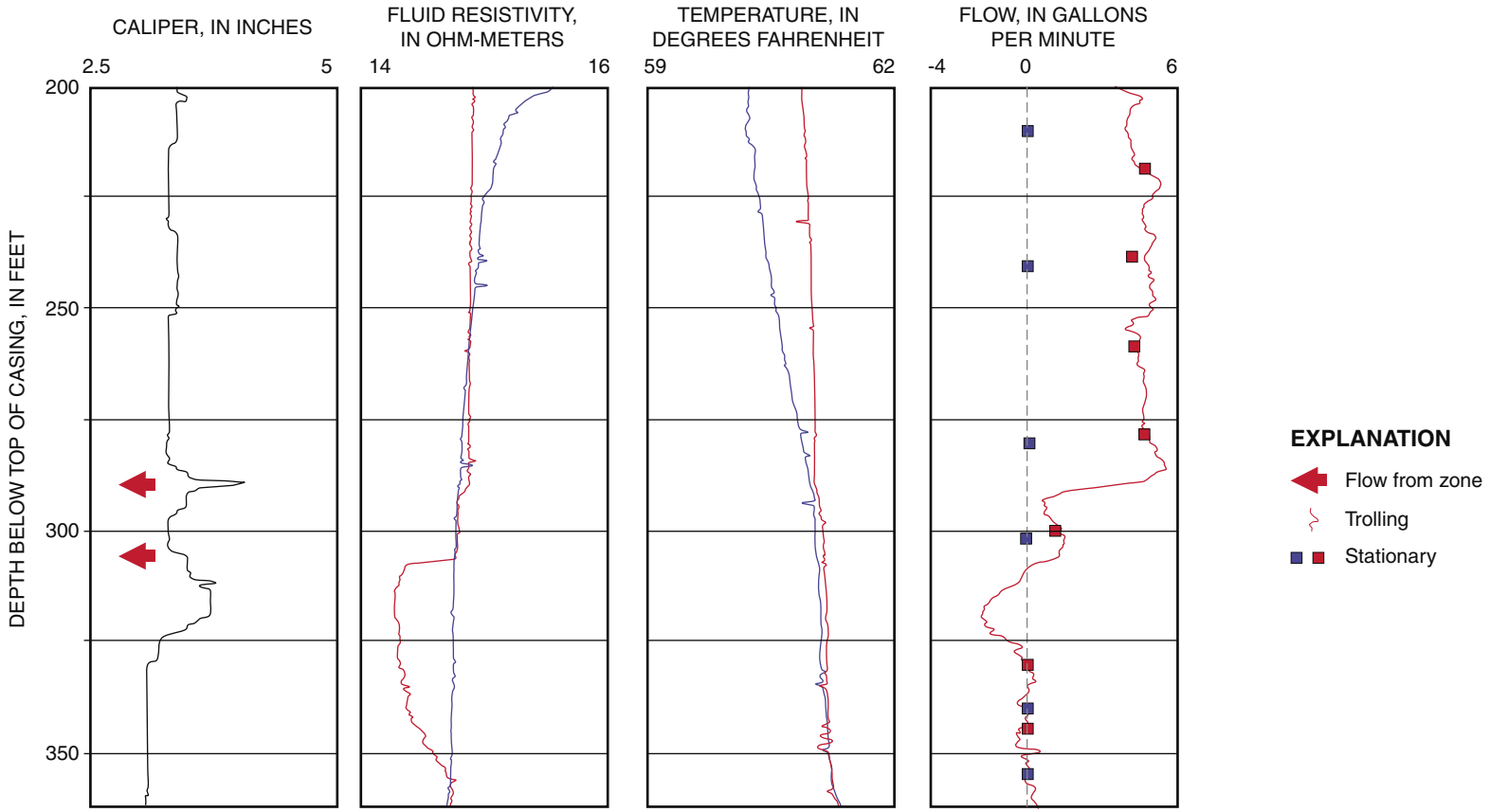

Fig. 16. Caliper, fluid-resistivity, temperature, and flowmeter logs of borehole RD-46B, Rocketdyne Santa Susana Field Laboratory, Ventura County, California (arrows indicate flow zones; blue indicates ambient conditions, red indicates pumped conditions; negative values indicate downflow, positive values indicate upflow).

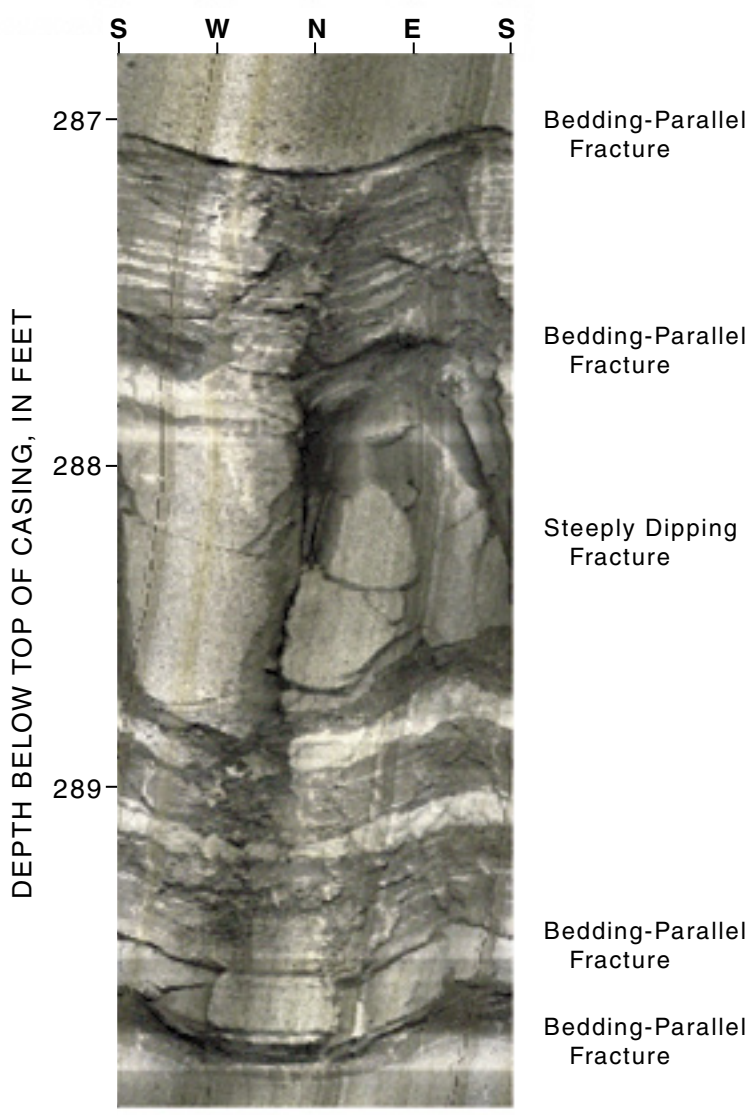

Figure 17. Optical-televiewer image of the flow zone near 289 feet in borehole RD-46B, Rocketdyne Santa Susana Field Laboratory, Ventura County, California.

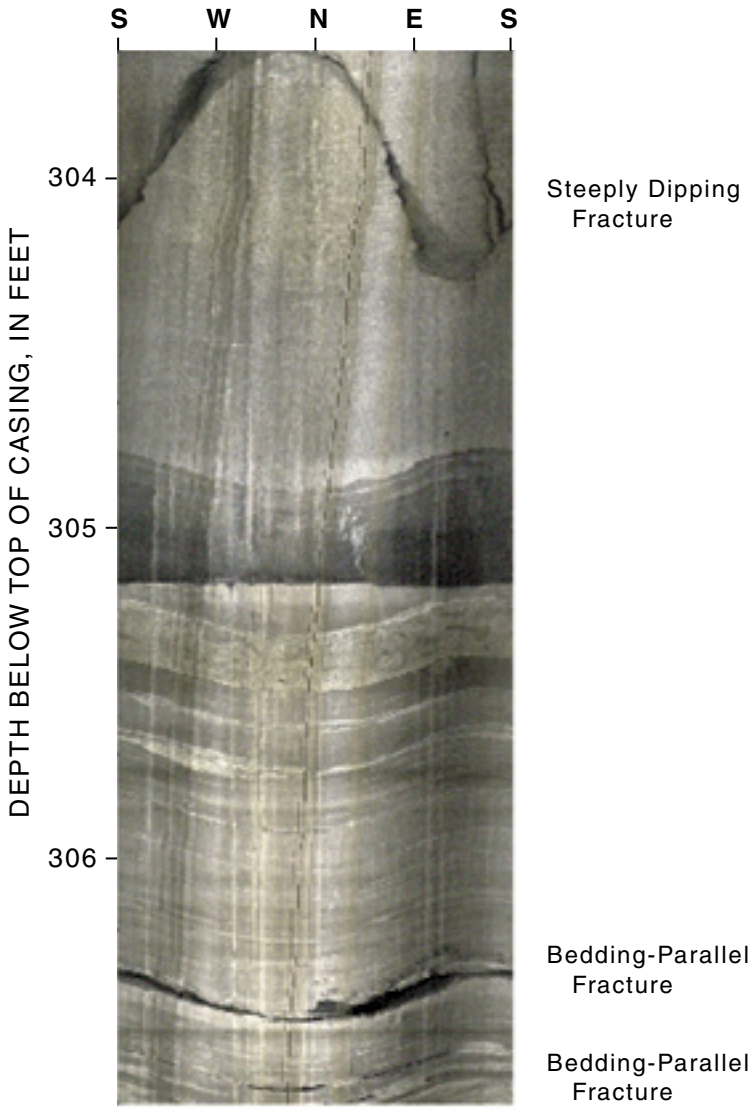

Figure 18. Optical-televiewer image of the flow zone near 306 feet in borehole RD-46B, Rocketdyne Santa Susana Field Laboratory, Ventura County, California.

Table 3. Midpoint depth, strike, and dip of bedding and fractures penetrated by borehole RD-46B, Rocketdyne Santa Susana Field Laboratory, Ventura County, California

[Strike is reported in azimuthal degrees, east of True North in "right hand rule" where the direction of the dip is to the right of the strike; blue indicates fractures in flow zones;-- indicates not determined.]

No.	Midpoint depth from top of casing, in feet	Type	Strike, in degrees	Dip, in degrees	Maximum apparent aperture, in inches
1	192.4	Bedding	320	22	--
2	218.2	Bedding	248	43	--
3	218.5	Bedding	233	49	--
4	219.1	Bedding	55	38	--
5	219.2	Bedding	60	26	--
6	222.8	Fracture	245	58	--
7	227.1	Bedding	253	34	--
8	232.3	Bedding	247	12	--
9	232.5	Bedding	220	38	--
10	235.2	Bedding	194	18	--
11	235.4	Bedding	90	0	--
12	236.1	Bedding	239	20	--
13	241.6	Fracture	205	2	--
14	242.3	Bedding	216	20	--
15	244.1	Fracture	246	32	0.7
16	247.0	Bedding	295	12	--
17	248.8	Bedding	252	19	--
18	254.1	Bedding	278	39	--
19	254.6	Fracture	234	22	0.2
20	256.0	Bedding	252	24	--
21	257.8	Bedding	262	24	--
22	258.0	Bedding	260	28	--
23	258.1	Fracture	252	26	0.2
24	258.4	Bedding	258	24	--
25	263.4	Bedding	252	20	--
26	264.4	Bedding	207	2	--
27	275.6	Fracture	125	49	0.1
28	275.6	Fracture	133	50	0.1
29	283.2	Bedding	223	14	--
30	286.2	Fracture	123	70	--
31	287.1	Fracture	245	26	0.2
32	287.1	Bedding	241	26	--
33	287.5	Bedding	232	30	--
34	287.7	Fracture	235	30	0.4

Table 3. Midpoint depth, strike, and dip of bedding and fractures penetrated by borehole RD-46B, Rocketdyne Santa Susana Field Laboratory, Ventura County, California -- continued

[Strike is reported in azimuthal degrees, east of True North in "right hand rule" where the direction of the dip is to the right of the strike; blue indicates fractures in flow zones;-- indicates not determined.]

No.	Midpoint depth from top of casing, in feet	Type	Strike, in degrees	Dip, in degrees	Maximum apparent aperture, in inches
35	288.2	Fracture	156	84	0.4
36	288.8	Bedding	214	31	--
37	289.1	Bedding	238	19	--
38	289.5	Fracture	229	24	0.2
39	289.7	Fracture	235	26	0.7
40	292.7	Bedding	229	33	--
41	292.8	Bedding	225	28	--
42	294.4	Bedding	232	24	--
43	296.0	Bedding	205	42	--
44	296.3	Bedding	208	46	--
45	297.7	Bedding	253	23	--
46	298.4	Fracture	340	77	0.5
47	298.5	Bedding	248	24	--
48	298.6	Fracture	242	26	--
49	299.2	Bedding	249	24	--
50	300.0	Bedding	246	24	--
51	301.2	Bedding	243	23	--
52	301.3	Bedding	220	22	--
53	301.7	Bedding	241	22	--
54	302.3	Bedding	244	22	--
55	302.9	Bedding	235	24	--
56	303.8	Fracture	42	70	0.1
57	304.8	Bedding	245	24	--
58	305.4	Bedding	241	23	--
59	306.4	Fracture	248	30	0.4
60	306.6	Fracture	249	25	0.1
61	307.1	Bedding	248	27	--
62	308.1	Bedding	251	21	--
63	308.2	Bedding	250	24	--
64	309.3	Bedding	244	27	--
65	309.9	Fracture	85	63	--
66	310.8	Bedding	246	30	--
67	311.5	Fracture	128	52	0.1
68	311.9	Bedding	242	22	--

Table 3. Midpoint depth, strike, and dip of bedding and fractures penetrated by borehole RD-46B, Rocketdyne Santa Susana Field Laboratory, Ventura County, California -- continued

[Strike is reported in azimuthal degrees, east of True North in "right hand rule" where the direction of the dip is to the right of the strike; blue indicates fractures in flow zones;-- indicates not determined.]

No.	Midpoint depth from top of casing, in feet	Type	Strike, in degrees	Dip, in degrees	Maximum apparent aperture, in inches
69	312.6	Fracture	231	28	0.4
70	312.7	Fracture	245	35	0.5
71	313.0	Fracture	241	30	0.2
72	313.5	Bedding	249	27	--
73	313.8	Fracture	230	25	0.1
74	313.9	Fracture	225	26	0.2
75	314.3	Bedding	243	31	--
76	316.2	Bedding	242	25	--
77	316.4	Fracture	234	28	0.1
78	316.8	Bedding	252	21	--
79	318.6	Bedding	246	20	--
80	320.0	Bedding	249	22	--
81	324.5	Bedding	247	24	--
82	325.5	Fracture	195	27	0.1
83	326.1	Fracture	248	34	0.1
84	326.3	Fracture	256	22	0.1
85	326.5	Fracture	262	47	0.2
86	326.8	Fracture	147	83	0.2
87	327.1	Fracture	255	22	0.1
88	328.6	Fracture	253	24	0.1
89	331.3	Bedding	260	19	--
90	332.3	Fracture	22	83	--
91	334.9	Fracture	251	25	0.1
92	335.9	Bedding	254	23	--
93	336.9	Fracture	269	25	0.1
94	339.7	Fracture	254	24	0.2
95	340.3	Fracture	257	37	--
96	341.7	Bedding	243	28	0.2
97	343.6	Bedding	248	26	--
98	344.2	Bedding	245	25	--
99	347.9	Fracture	246	26	0.2
100	348.9	Bedding	236	28	--
101	352.5	Bedding	244	22	--
102	356.6	Bedding	249	27	--
103	363.3	Bedding	247	26	--

SUMMARY

The advanced geophysical logging methods used in this investigation provided an efficient means to characterize the geology and hydrology of three boreholes completed in fractured-sedimentary bedrock at the Rocketdyne Santa Susana Field Laboratory in southern Ventura County, California. The results of the geophysical logging provided insights useful for the geohydrologic characterization of the aquifer including the enhancement of the value of information collected by other borehole methods.

Boreholes RD-35B, RD-46A, and RD-46B penetrate a sequence of interbedded sandstone and mudstone, with bedding striking 220 to 250° and dipping 15 to 40° to the northwest. Fractures intersected by the boreholes include fractures that parallel bedding and fractures with variable strike that dip moderately to steeply. Most fractures appear partly open to open with maximum apparent opening widths that range from 0.1 to 3.8 in.

Flow zones were detected at depths of 201 and 312 ft in borehole RD-35B; 95, 119, and 132 ft in borehole RD-46A; and 289 and 306 ft in borehole RD-46B. Four of the flow zones consist of both bedding-parallel fractures and moderately to steeply dipping fractures, two of the zones consist of only steeply dipping fractures, and one zone consists of a single bedding-parallel fracture.

Under ambient conditions, slight downward flow between the flow zones in borehole RD-35B was identified from fluid and flowmeter logging. The fluid temperature log from RD-46B indicates that ambient flow involving the transmissive zone at 290 ft could exist.

When pumped at 3.3 to 4.9 gal/min for 1.5 to 3 h, specific capacities of the boreholes ranged from 0.33 to 0.55 (gal/min)/ft. About 75 to more than 90 percent of the measured flow under pumped conditions was produced by only one of the flow zones in each borehole. Borehole water above the flow zones was purged within 0.75 h from the start of pumping in borehole RD-46B and between 0.5 and 1.5 h after the start of pumping in borehole RD-35B. Borehole water above the flow zones was not purged in borehole RD-46A after 3 h of pumping.

REFERENCES

Keys, W. S., 1990, Borehole geophysics applied to ground-water investigations: U. S. Geological Survey Techniques of Water-Resources Investigations, book 2, chap. E2, 150 p.

Lane, J. W., Jr., Haeni, F. P., and Williams, J. H., 1994, Detection of bedrock fractures and lithologic changes using borehole radar at selected sites, in Proceedings of the Fifth International Conference on Ground Penetrating Radar, Kitchener, Ontario, Canada, June 12-16, 1994: Waterloo, Ontario, Waterloo Centre for Groundwater Research, p. 557-592.

Paillet, F. L., 1998, Flow modeling and permeability estimation using borehole los in heterogeneous fractured formations: Water Resources Research, v. 34, no. 5, p. 997-1010.

Sterling, S. N., 1999, Comparison of discrete depth sampling using rock core and a removable multilevel system in a TCE contaminated fractured sandstone: MS Thesis, Department of Earth Sciences, University of Waterloo, Waterloo, Ontario, Canada, 108 p.

Williams, J. H. and Conger, R. W., 1990, Preliminary delineation of contaminated water-bearing fractures intersected by open-hole bedrock wells: Ground Water Monitoring Review, v. 10, no. 3, p. 118-126.

Williams, J. H., Lapham, W. W., and Barringer, T. H., 1993, Application of electromagnetic logging to contamination investigations in glacial sand and gravel aquifers: Ground Water Monitoring and Remediation Review, v. 13, no. 3, p. 129-138.

Williams, J. H. and Lane, J. W., Jr., 1998, Advances in borehole geophysics for ground-water investigations: U. S. Geological Survey Fact Sheet 002-98, 4 p.

Young, S. C. and Pearson, H. S., 1995, The electromagnetic borehole flowmeter – description and application: Ground Water Monitoring and Remediation Review, v. 15, no. 4, p. 138-147.

This report and additional earth science information can be found on the World Wide Web at http://ny.usgs.gov

USGS
science for a changing world

For more information contact:
District Chief
U.S. Geological Survey/WRD
425 Jordan Road
Troy, NY 12180

Copies of this report can be purchased from:
U.S. Geological Survey
Branch of Information Services
Box 25286
Denver, CO 80225-0286